

Lawrence Berkeley National Laboratory

Lawrence Berkeley National Laboratory

Title

EXPERIMENTAL EVIDENCE AND THEORETICAL IMPLICATIONS OF FLUCTUATIONS IN DEEP INELASTIC HEAVY ION COLLISION

Permalink

<https://escholarship.org/uc/item/2cw7r3vf>

Author

Moretto, L.G.

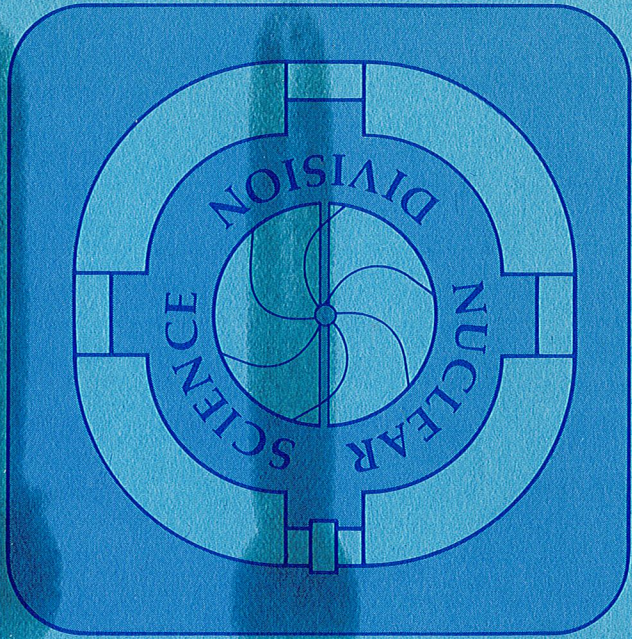
Publication Date

1981-04-01

Peer reviewed

LBL-12596 c.2

Prepared for the U.S. Department of Energy under Contract W-7405-ENG-48



~~RESTRICTED~~
LABORATORY

JUL 2 1981

April 1981

RECEIVED
LAWRENCE
BERKELEY
LABORATORY

L. G. Moretto

EXPERIMENTAL EVIDENCE AND THEORETICAL IMPLICATIONS
OF FLUCTUATIONS IN DEEP INELASTIC HEAVY ION COLLISION

To be presented at the Europhysics Conference on
Nuclear Physics, Hvar, Croatia, Yugoslavia,
June 29-July 3, 1981

Lawrence Berkeley Laboratory
UNIVERSITY OF CALIFORNIA



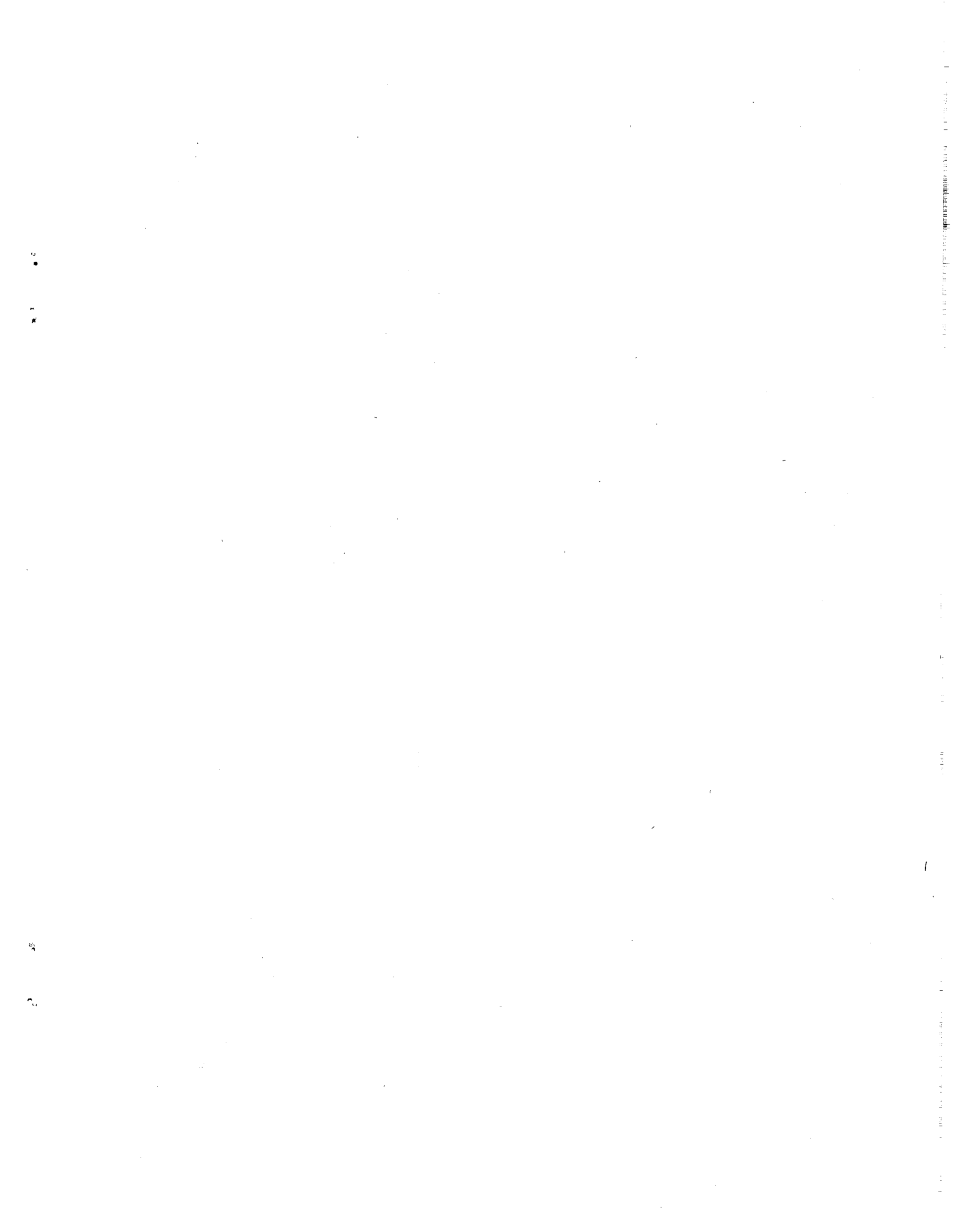
LBL-12596 c.2

Experimental Evidence and Theoretical Implications of
Fluctuations in Deep Inelastic Heavy Ion Collisions

L. G. Moretto

Nuclear Science Division, Lawrence Berkeley Laboratory
University of California, Berkeley, CA 94720

This work was supported by the Director, Office of Energy
Research, Division of Nuclear Physics of the Office of High Energy
and Nuclear Physics and by Nuclear Sciences of the Basic Energy
Sciences Program of the U.S. Department of Energy under Contract
W-7405-ENG-48.



L. G. MORETTO

Nuclear Science Division, Lawrence Berkeley Laboratory
University of California, Berkeley, CA 94720

Abstract: The role of fluctuations in deep inelastic collisions is discussed. The relevance of the statistical equilibrium limit to the description of substantially relaxed degrees of freedom is assessed. The effects of fluctuations are considered specifically for the following processes: a) the correlation between entrance-channel angular momentum and exit-channel kinetic energy; b) the sharing of the dissipated kinetic energy between the two fragments; c) the alignment of the fragment angular momentum. It is found that statistical fluctuations play a major role and that the statistical equilibrium limit seems to have been reached in a number of instances.

1. Introduction

Traditionally nuclear physics has developed within the framework of quantum mechanics and one could not work on the former without knowing the latter. When the heavy ion field was opened, classical mechanics struck back with a vengeance. The old school was confronted with hopelessly complicated and unworkable models cast in the frame of quantum mechanics, while the new school gloated over their elegant (and workable!) equations of motion. In the words of an embittered representative of the old school "...the barbarians have come." But, as the time went by, the new school started getting old, the experiments became more precise and pointed, and the demands from theories more exacting. It was appreciated soon that a fully deterministic picture of deep inelastic reactions was nothing but a dream. Nuclei are small, after all, even in terms of their number of degrees of freedom, and they are made even smaller by the Pauli principle that freezes most of the nucleons in momentum space. It became soon apparent that fluctuations of either quantum or statistical nature could be large and comparable to the mean values and thus would play a major role. One can appreciate this point, by just comparing an experimental Wilczynski diagram with a classical trajectory calculation or with a TDHF calculation (classical mean-field theory). Clearly, the theory is missing a big, if not the major, point of the physics. Fluctuations can find their origin either in quantal or in statistical effects, and may be associated either with equilibrium or nonequilibrium processes. Their relevance becomes preeminent when the temperature T (or the phonon $\hbar\omega$) becomes comparable with the potential energy variations ΔV along a given collective coordinate. When this occurs, the second and higher moments become important. Furthermore, spectral distributions are frequently controlled, more or less directly, by fluctuations (e.g., kinetic energy spectra). Finally, the dissipation-fluctuation theorem states that fluctuations are the inevitable consequence of

This means that, while, after one relaxation time, the centroid is still 37% of the initial distance from equilibrium value. In other words, the width grows rapidly towards its equilibrium value independently of the starting point and can approach its limiting value while the mean may still be quite far away from equilibrium. Even after only one-half the relaxation time, the width is already 82% of its equilibrium value, while the mean is still 60% of the initial distance from equilibrium. The impact of this simple observation is profound. If the system has any inclination at all to relax towards equilibrium, we can estimate the fluctuations quite reliably by means of the equilibrium fluctuations without worrying too much about the time dependence of the process. Of course, the time dependence is a very important feature that deserves to be studied in detail. However, if we are concerned about the role of fluctuations and about their ability to scramble the experimental picture, a thorough investigation of the equilibrium limit is the most economical way to obtain information about this problem. In the rest of my talk, I would like to give some examples of the role of fluctuations in deep inelastic processes. In

$$\frac{x}{x_0} = e^{-t} = 0.368 \quad ; \quad \frac{\sigma_{\text{equil}}}{\sigma} = 1 - \frac{1}{2} e^{-2} = 0.93$$

where B is the "mobility" of the system. After one relaxation time $t = 1/CB$, we have:

$$\sigma^2 = \frac{C}{B} (1 - e^{-2CBt})$$

(1)

$$x = x_0 e^{-CBt}$$

If we start from $x = x_0$ at $t = 0$ with a delta function distribution, after a time t the distribution is a Gaussian with centroid and width given by:

$$V(x) = \frac{1}{\sqrt{2}} e^{-\frac{x^2}{2}}$$

From this point onward I shall limit myself to the discussion of equilibrium statistical fluctuations. The true reason for this choice could be, as one may suspect, laziness. Fortunately, there is a marvelous rationalization that may protect me, to some extent, from accusations of this sort. Let us assume that the approach to equilibrium is controlled by a diffusive process as described by the Master Equation or by the Langevin equation. Furthermore, let us assume that the system is harmonically bound along the coordinate under consideration, namely:

The question of quantal versus thermal fluctuations is an interesting one. The former has been pursued theoretically by the Copenhagen group¹; the latter has such a solid historical tradition in the field of the compound nucleus decay that it is not in need of strong justification. The question of nonequilibrium vs. equilibrium fluctuations is worth debating in some greater detail.

From this point onward I shall limit myself to the discussion of equilibrium statistical fluctuations. The true reason for this choice could be, as one may suspect, laziness. Fortunately, there is a marvelous rationalization that may protect me, to some extent, from accusations of this sort. Let us assume that the approach to equilibrium is controlled by a diffusive process as described by the Master Equation or by the Langevin equation. Furthermore, let us assume that the system is harmonically bound along the coordinate under consideration, namely:

particular, I shall discuss: a) fluctuations in the exit channel kinetic energy and the correlation (or the lack of it) between it and the entrance channel angular momentum, b) fluctuations in the partition of the dissipated energy between the two fragments and their possible effects in the emission of fast particles, and c) fluctuations in the spin components of the fragments and the resulting spin misalignment as observed from sequential fission and γ -ray decay of the fragments. Space and time restrictions prevent me from discussing other equally interesting subjects, like isospin fluctuations. The curious component of the audience can find some satisfaction in the available literature.²⁾

2. Correlation between exit-channel kinetic energy and entrance-channel angular momentum

One of the oldest dreams of the practitioners in this field has been that of inferring the entrance-channel angular momentum from some easily measurable exit-channel observable, like the kinetic energy. While some correlation between these quantities is obviously present, especially in the quasi-elastic region, fluctuations of a various nature tend to spoil it to a serious degree. We are going to discuss two sources of fluctuations relevant to this problem: a) the coupling of the orbital motion to a thermally excited wiggling mode;³⁾ and b) the effect of random shape fluctuations at scission.

2a) COUPLING OF THE ORBITAL MOTION TO ONE WRIGGLING MODE

Let us consider the simple analytical case of two equal touching spheres with one wiggling mode³⁾ coupled to the orbital motion. The exit channel kinetic energy above the Coulomb barrier is:

$$E = \frac{\lambda^2}{2} + \frac{2\mu d^2}{2} \quad (2)$$

where λ is the exit-channel orbital angular momentum, μ is the reduced mass, and d is the distance between centers, equal to the sum of the radii. The total rotational energy is:

$$E_R = \frac{\lambda^2}{2} + \frac{4J}{I} - \frac{2J}{I} \quad (3)$$

where I is the entrance channel angular momentum, J is the moment of inertia of one of the two spheres, and $J^* = I(\omega^2) - I + (2J) - I$ or $J^* = 10/7 J$. In the limit of thermal equilibrium, the λ distribution is:

$$P(\lambda)d\lambda = (2\pi J^* T)^{-1/2} \exp - \frac{\lambda^2}{2} - \frac{2J^* T}{I} - \frac{2J T}{I} + \frac{8J^2 T}{2J^*} \quad (4)$$

where T is the temperature. Introducing a Zeldi weight and the dimensionless variables $\epsilon = E/T$, $\lambda = I/(J T) I/2$, we obtain the distribution function:

Since λ_T is typically 100-200 \hbar^2 , we have widths in the entrance channel angular momentum

$$17\hbar \leq \sigma \leq 24\hbar$$

$$40\hbar \leq \text{FWHM} \leq 56\hbar$$

$$\sigma^2 = \frac{14}{5}, \text{ independent of } \epsilon; \quad (7)$$

while the width is given by

$$\lambda = \frac{14}{\sqrt{\epsilon}} \text{ from simple dynamics,}$$

to be compared with

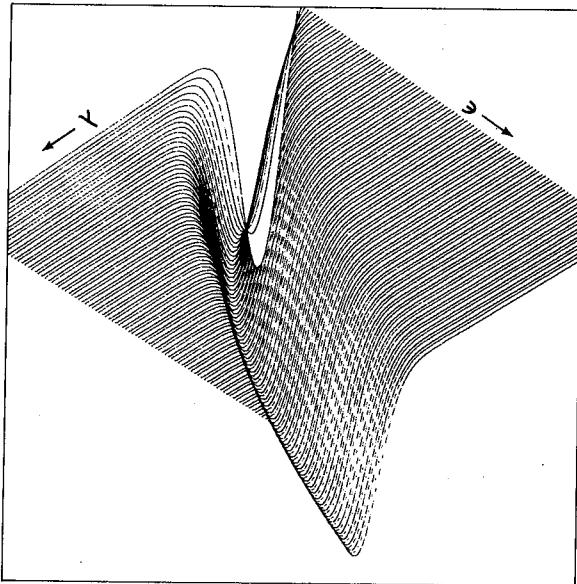
$$\lambda = \frac{14}{\sqrt{\epsilon}} \left[1 + \sqrt{1 + \frac{4}{7\epsilon}} \right] \quad (6)$$

At constant ϵ (a fixed cut in the exit channel kinetic energy), the most probable value of λ is:

in eq. 5.

Fig. 1. Two-dimensional plot of the distribution function given

XBL 915-2266



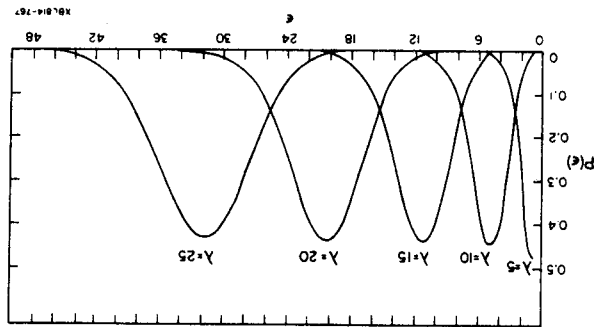
The properties of this distribution function can be observed in the two-dimensional plot in fig. 1 and can be summarized as follows.

$$P(\epsilon, \lambda) d\epsilon d\lambda \propto \frac{\lambda}{\sqrt{\epsilon}} \exp \left[-\frac{7}{2\epsilon} - \sqrt{\frac{5}{2}} \lambda \sqrt{\epsilon} + \frac{28}{5} \lambda^2 \right] d\epsilon d\lambda \quad (5)$$

$$P(\epsilon) \propto \frac{1}{\sqrt{\epsilon}} \left[e^{-\frac{\sqrt{\epsilon}}{2}} \left(1 - e^{-\frac{28}{5}\lambda\sqrt{\epsilon}} + \sqrt{\frac{2}{5}}\lambda\sqrt{\epsilon} + \sqrt{\frac{2}{5}}\lambda\sqrt{\epsilon} \right) \right. \\ \left. + \sqrt{\frac{2}{5}}\lambda\sqrt{\epsilon} \left(\sqrt{\frac{2}{5}}\lambda\sqrt{\epsilon} + \text{erf} \left(\sqrt{\frac{2}{5}}\lambda\sqrt{\epsilon} \right) \right) \right] \quad (11)$$

The integration yields:
 We conclude this subject by calculating the kinetic energy distribution integrated over angular momentum from 0 to λ_{mx} .

Fig. 2. Kinetic energy distributions for various values of the entrance-channel angular momentum.



Examples of distributions in ϵ at fixed λ are shown in fig. 2. The conclusion is that a sizeable mixing of entrance channel λ -waves is predicted for a fixed exit-channel kinetic energy by invoking just one thermally-excited wriggling mode.

For an entrance channel angular momentum $I \approx 240$ h, $\sqrt{T} \approx 144$ h^{1/2}, $T \approx 3$ MeV, one obtains
 $\sigma = 10$ MeV, $\Gamma_{FWHM} = 23.5$ MeV,
 while, for $I = 360$ h (rms for Ho + Ho at 8.5 MeV/A) one obtains:
 $\sigma = 15$ MeV, $\Gamma_{FWHM} = 36$ MeV.

$$\frac{\sigma}{\epsilon} = \frac{(1/2 + 5/14\lambda^2)^{1/2}}{1/2 + 5/28\lambda^2} \approx 2 \sqrt{\frac{14}{5}} \frac{\lambda}{1} \quad (10)$$

and

$$\sigma^2 = \frac{4}{9} \left(\frac{1}{2} + \frac{14}{5} \lambda^2 \right) \quad (9)$$

while the width is:

$$\epsilon = \frac{7}{2} \left(\frac{1}{2} + \frac{28}{5} \lambda^2 \right) \quad (8)$$

For an infinitely sharp cut in the exit channel kinetic energy. At constant λ (a fixed entrance-channel angular momentum), the average kinetic energy over the barrier is:

It was realized, very early in the history of heavy ion reactions, that the observed sub-Coulomb emission of deep-inelastic fragments is due to their sizeable deformation at the scission point. The reasonably flat dependence of the total potential energy at scission as a function of deformation, together with the rather steep dependence of the two-fragment Coulomb interaction, leads to the possibility of fairly large

2b) SHAPE FLUCTUATIONS IN THE EXIT CHANNEL

In other words, we have a rectangular distribution. Examples of such distributions are also shown in fig. 3.

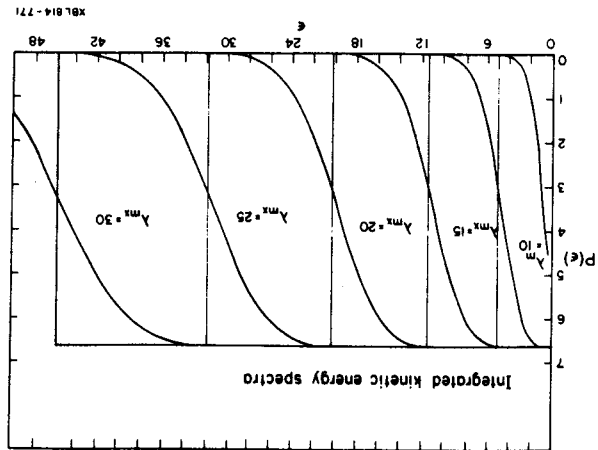
which implies $E = \frac{1}{2} \frac{2\mu d^2}{I} = \frac{49}{25} \frac{2\mu d^2}{I}$

then $P(E) dE \propto dI^2 \propto dE$ or, more precisely, $P(\lambda) d\lambda = K d\lambda^2 = K d\lambda^2 = K' dI^2$,
 But, from the entrance channel distribution, we have $dE \propto dI^2$.

$K d\lambda \leq \frac{98}{5} \lambda^2 m_x$
 $0 < \frac{98}{5} \lambda^2 m_x$

The kinetic energy over the barrier is:

Fig. 3. Angular-momentum-integrated kinetic energy distributions for different values of the maximum angular momentum. The box-like distributions defined by the vertical lines are obtained by eliminating fluctuations.



Plots of this distribution for different values of λ_{mx} are shown in fig. 3. In order to appreciate better this result, we can calculate the corresponding distribution in the absence of fluctuations ($T = 0$) in the limit of rigid rotation:

shape fluctuations at scission with a resulting amplification of the fluctuations in the kinetic energy at infinity.⁴⁾ For sake of simplicity, let us model the system at scission as composed of two equal and equally deformed spheroids in contact. The relevant total potential energy is

$$V_T = V_S(\epsilon) + V_C(\epsilon) + V_{Rot}(I, \epsilon) \quad (12)$$

where V_S , V_C , V_{Rot} are the surface, Coulomb, and rotational energy, respectively; ϵ is the common deformation of the spheroids; and I is the angular momentum. In our model the potential energy has a minimum at a deformation ϵ_0 defined by

$$\frac{\partial V_T}{\partial \epsilon} = 0$$

The potential energy can be expanded quadratically about the minimum as

$$V_T \approx V_0 + k(\epsilon - \epsilon_0)^2 \quad (13)$$

Similarly, the resulting kinetic energy at infinity is given by

$$E_{kin} = V_C^*(\epsilon) + \frac{2I^2}{\lambda(\epsilon)^2} \quad (14)$$

where V_C^* is the two-fragment Coulomb interaction, $\lambda(\epsilon)$ is the orbital angular momentum at scission determined from the rigid rotation condition, and d is the center-to-center distance. A linear expansion in ϵ about ϵ_0 leads to

$$E_{kin} \approx E_0^{kin} + c(\epsilon - \epsilon_0)$$

From fig. 4, K_{lin} one sees that a small (energy-wise) fluctuation at

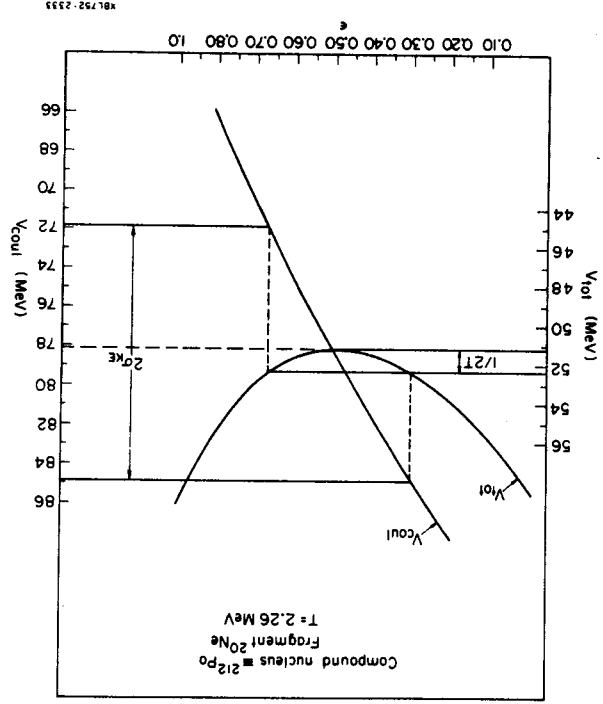


Fig. 4. Amplification of fluctuations at scission illustrated for a ^{20}Ne emitted by the compound system ^{212}Po .

Fig. 5. Kinetic energy spectra for various values of the entrance-channel angular momentum for the system Fe + Fe.

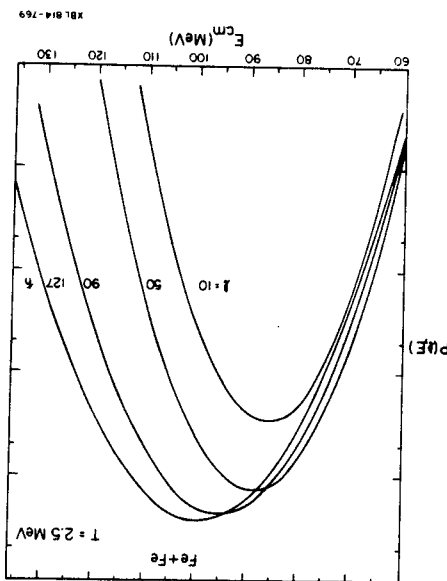
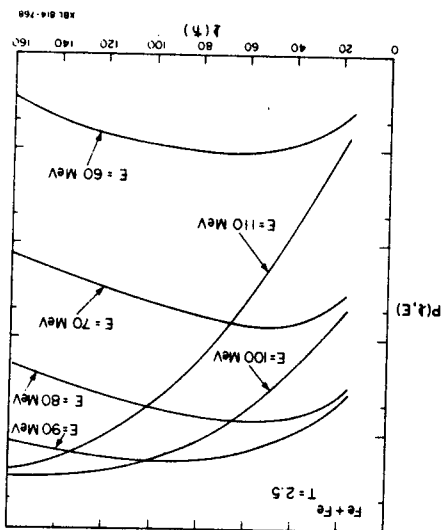


Fig. 6. Entrance-channel angular momentum distributions for various values of exit-channel kinetic energies.



Certainly a great deal of the width in the final kinetic energy distribution arises from this effect. Even more interesting is the fact that the large spread in final kinetic energy is associated with a fixed total angular momentum. Of course, this feature has the effect of spreading any given λ -wave over a very broad range of kinetic energies, thus making the correlation between exit-channel kinetic energy and entrance-channel angular momentum very problematic.

As an example, let us consider the system Fe + Fe. In fig. 5 the kinetic energy distributions are shown for a set of λ values. While the centroid of the distribution moves towards higher values with increasing λ , the width also increases, leading to a dramatic overlap of distributions with widely different λ -values. Most interesting are the entrance-channel angular momentum distributions for a variety of exit-channel kinetic energies shown in fig. 6. The distributions are so broad that at any kinetic

$$P(E_{kin}) \propto \exp - \frac{pT}{(E_{kin} - E_0^{kin})^2} \quad (16)$$

where p is called the amplification parameter.⁴ The exit-channel kinetic energy distribution is, in fact, approximately a Gaussian

$$\sigma_{kin}^2 = \frac{c^2}{2T} = \frac{2}{pT} \quad (15)$$

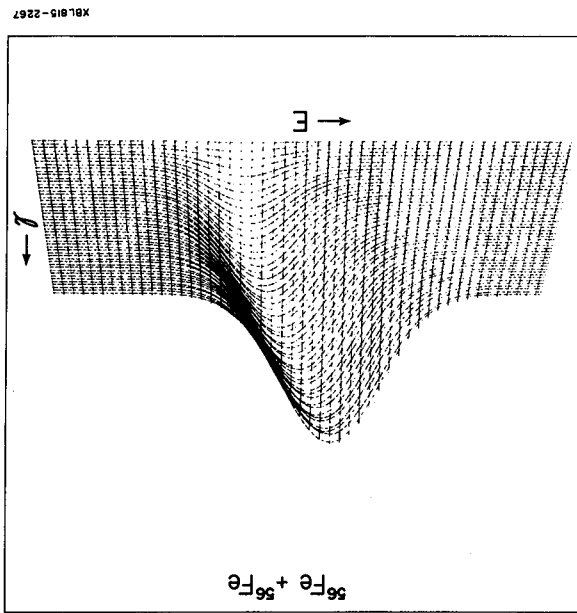
scission, of the order of $1/2T$ in the thermal limit, leads to an amplified fluctuation in the final kinetic energy, so that

The equilibrium of excitation energy between the partners in a deep-inelastic collision (DIC) appears to occur on a very short time scale. This fast equilibrium seems to be required by the experimental observation that the mean number of evaporated particles from coincident reaction products is indicative of a splitting of the total dissipated energy in proportion to the fragment masses,⁵⁻⁷ as required by the thermal equilibrium condition. Moreover, this proportionality is found for the entire range of dissipated energy, up to the smallest energy losses⁸⁻¹⁰ (i.e., the shortest collision times). Thus the thermalization time must be shorter than the shortest interaction times. A further check of complete statistical equilibrium can be

3. Statistical sharing of energy between the two fragments

In conclusion, we have seen how the two processes described in a) and b) have the effect of spoiling the correlation between entrance-channel angular momentum and exit-channel kinetic energy. It is easy to think of other possible causes of similar nature. Still, in certain cases the picture may be made less dismal if the cross section is substantially spread-out in angle. Then we can hope for a correlation between exit-channel λ -value and angle. However, on one hand, this correlation is lost when strong focusing is present; on the other, the correlation between exit-channel λ -value and entrance-channel angular momentum still remains hazy, as shown in a).

Fig. 7. Two-dimensional plot of the emission probability as a function of entrance-channel angular momentum and exit-channel kinetic energy.



energy the whole λ -wave spectrum is substantially sampled. The overall features of the distribution are shown by the two-dimensional plot in fig. 7.

$$\frac{1}{2} = - \frac{d}{dx} \ln P(x) = \frac{d}{dx} \ln \left(\frac{1}{A_1} \right) + \frac{d}{dx} \ln \left(\frac{1}{A_2} \right) \quad (21)$$

$$P(x) dx \propto e^{-\frac{(x-x_0)^2}{2\sigma^2}} \quad (20)$$

The expansion of the logarithm of the probability distribution about the maximum up to 2nd order gives a Gaussian:

$$\frac{E_1^*}{A_1} = \frac{E_2^*}{A_2} = \frac{E - x}{x} \quad (19)$$

The terms on the right-hand side of eq. 18 are the reciprocals of the fragments' temperatures and their equality immediately requires the excitation energy to divide in proportion to the mass ratio:

$$\frac{d}{dx} \ln P(x) = 0 = \frac{d}{dx} \ln P_1(x) + \frac{d}{dx} \ln P_2(E - x) = \frac{1}{x} - \frac{1}{E - x} \quad (18)$$

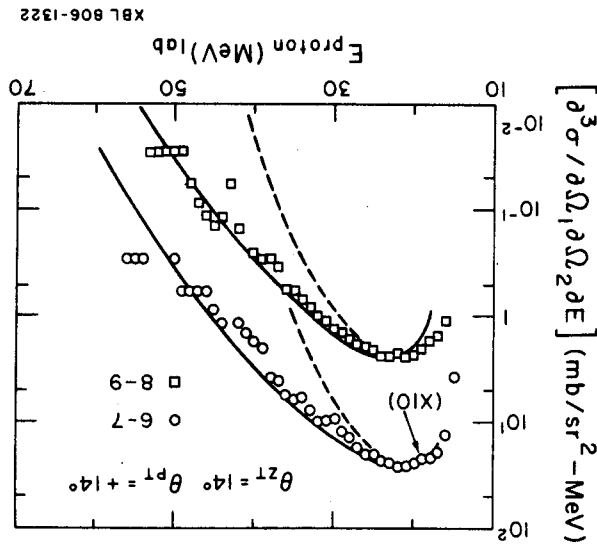
The equilibrium condition is given by:

$$P(x) dx \propto P_1(x) P_2(E - x) dx \quad (17)$$

In this section we evaluate the magnitude of statistical fluctuations in the energy partition in DIC and explore two avenues through which the calculated fluctuations can manifest themselves, namely neutron energy spectra and evaporated neutron number. 16) We find that these two observables are complementary in that statistical fluctuations have a large effect on the neutron energy spectra when the mass asymmetry is large but have a relatively small effect for equal fragments. Fluctuations also introduce a covariance in the number of evaporated nucleons which is most prominent for equal fragments. The statistical weight associated with a given partition of the total excitation energy, E, between two fragments in statistical equilibrium is proportional to the product of their level densities:

made by observing statistical fluctuations in the division of the excitation energy between the two fragments. 11) Such fluctuations will have important consequences for the reaction products. The effects of a fluctuating excitation energy division on evaporation spectra and the dissolving of pre-equilibrium components have been described recently by Schmitt et al. 12) Fluctuations in the excitation energies of the primary reaction products from DIC also must be taken into account in measurements of the isobaric width of the primary fragments. 13-15) The effect of fluctuations on the isobaric widths have been noted but also neglected (e.g., ref. 14) or treated as a free parameter (e.g., ref. 14).

Fig. 8. Proton spectra in coincidence with deep inelastic processes for the reaction $^{20}\text{Ne} + \text{natCu}$. The dashed lines are evaporation calculations without fluctuations in the energy partition. The solid lines incorporate the fluctuations. A less direct, but more dramatic effect of excitation energy fluctuations can be seen in the number of nucleons evaporated from the pair of DIC fragments. An anticorrelation in the excitation energies of reaction partners naturally arises when the total excitation energy is held constant. The covariance of the number of emitted neutrons from DIC partners was investigated with a simple Monte Carlo code. The division of the excitation energy between symmetric fragments ($A = 100$) was either fixed or picked



XBL 806-1322

where a_1 and a_2 are the level density parameters of the fragments.
 A direct way in which any fluctuations in the excitation energy of DIC fragments can be observed is in the energy spectra of evaporated nucleons.
 For a very asymmetric system, the magnitude of the fluctuations is comparable to the total excitation energy of the light fragment and therefore produces an important change in the spectrum.
 As an applied example, fig. 8 shows the proton spectra in coincidence with deep inelastic fragments for the reaction $\text{Ne} + \text{Cu}$ at 252 MeV.¹²⁾ While the hard spectrum could be attributed to prompt emission, it is in fact explained quite simply by energy fluctuations (solid lines) while it is not consistent with fixed energy splitting between fragments (dashed lines).

$$\sigma^2 = 2\pi^3 \frac{a_1 a_2}{a_1 + a_2} \quad (22)$$

we obtain for the width:
 where C_{V1} and C_{V2} are the heat capacities of the two fragments (for a Fermi gas $C_V = 2aT$ at a temperature T). On substitution

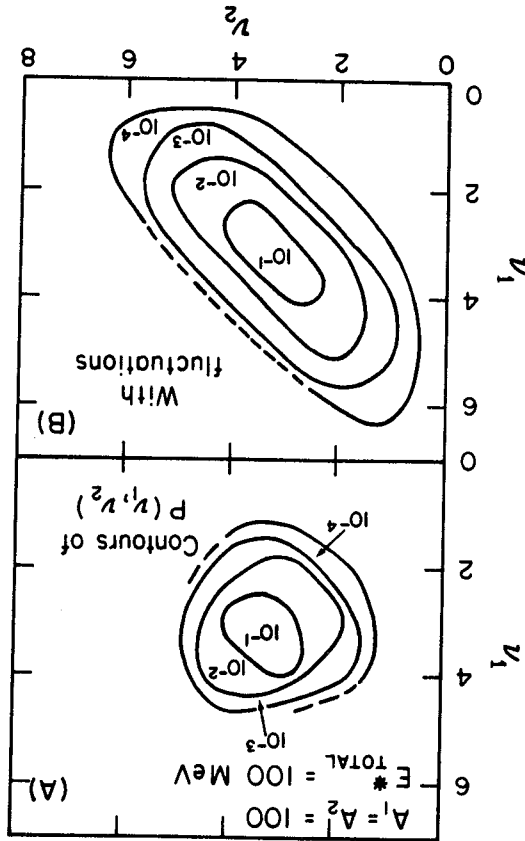
Let us consider a frame of reference where the z axis is parallel to the entrance-channel angular momentum, the x axis is parallel to the recoil direction of one of the fragments, and the y axis is perpendicular to the z, x plane.

4a) THE STATISTICAL MODEL

4. Fluctuations in the spin components of the fragments

Fig. 9. Probability distribution for the number of neutrons emitted by the two fragments for a Q-value of -100 MeV. The fluctuations in the energy partition are incorporated in B.

XBL 808-1552



at random in proportion to eq. 17. The two fragments were then allowed to emit neutrons until the nuclei had cooled to less than $B_N + 2T'$, where B_N is the liquid drop neutron binding energy and T' is the temperature after emission of the previous neutron. The probability contours for emission of v_1 neutrons from fragment 1 and v_2 neutrons from fragment 2 are shown in fig. 9. When the fluctuations are turned on, a strong correlation between v_1 and v_2 is introduced.

If the intermediate complex is assumed to have the shape of two equal touching spheres, the angular-momentum-bearing normal modes are easily identifiable. We shall call them "bending," "doubly degenerate," "twisting" T_w (degenerate with bending), "wiggling" W (doubly degenerate) and "tilting" T_t . In a recent work, the statistical mechanical aspects of the excitation of these modes have been studied in detail.³ Here we report only the relevant conclusions. The thermal excitation of these collective modes leads to Gaussian distributions in the three angular momentum components I_x, I_y, I_z , namely:

$$P(\vec{I}) \propto \exp - \left(\frac{I_x^2}{2\sigma_x^2} + \frac{I_y^2}{2\sigma_y^2} + \frac{I_z^2}{2\sigma_z^2} \right) \quad (23)$$

where:

$$\begin{aligned} \sigma_x^2 &= \sigma_w^2 + \sigma_{T_t}^2 = \frac{1}{2} J T + \frac{10}{7} J T = \frac{5}{6} J T \\ \sigma_y^2 &= \sigma_B^2 + \sigma_w^2 = \frac{1}{2} J T + \frac{14}{5} J T = \frac{7}{6} J T \\ \sigma_z^2 &= \sigma_B^2 + \sigma_w^2 = \frac{1}{2} J T + \frac{14}{5} J T = \frac{7}{6} J T \end{aligned} \quad (24)$$

The quantity J is the moment of inertia of one of the two touching spheres, and T is the temperature. Notice that the variances along the three coordinates are almost equal. Frequently the degree of alignment of the fragment spins is expressed in terms of the alignment parameter P_{zz} = $3/2 \langle I_z^2 / I^2 \rangle - 1/2$. If $\sigma_x = \sigma_y = \sigma_z = \sigma$ it is possible to express the alignment parameter P_{zz} in terms of σ and the average z-component of the fragment angular momentum I_z as follows:

$$P_{zz} = \frac{3}{2} \frac{I_z^2}{I^2} - \frac{1}{2} = \frac{3}{2} \frac{I_z^2}{I_x^2 + I_y^2 + I_z^2} - \frac{1}{2} \quad (25)$$

4b) GAMMA RAY ANGULAR DISTRIBUTIONS

The fragment angular momentum is removed mainly by stretched E2 decay. The alignment of the angular momentum should be manifested in the gamma ray angular distributions, whose sharpness should decrease with increasing misalignment. If the distribution of the angular momentum components I_x, I_y, I_z is statistical, it is straightforward to derive analytical expressions for the angular distributions.¹⁷

If one assumes $\sigma_x^2 = \sigma_y^2 = \sigma_z^2 = \sigma^2$ then an exact

result can be derived.

The ratio of in-plane to out-of-plane γ -ray yield ("anisotropy") for energies between 0.6 and 1.2 MeV is also shown in fig. 10 (bottom). This anisotropy rises with increasing spin transfer; it peaks at a value of 2.2, slightly before the spin saturates, and then drops to near unity for large Q -values. The initial rise of the anisotropy with increasing Q -value indicates that during the early stages of energy damping there is a rapid buildup of aligned spin. The subsequent fall observed at larger Q -values suggests that the aligned component of spin has saturated or is decreasing, whereas randomly oriented components continue to increase, causing a significant decrease in the alignment of the fragments' spin.

Figure 11 shows experimental values of the anisotropy for E_1 greater than 0.6 MeV compared to several stages of the model shown. The primary fragment spin obtained from emission (solid line). The primary fragment spin obtained from M_1 upon Q -value for three angles. Figure 10 (middle) shows the dependence of the γ -ray multiplicity are strongly enriched in E2 transitions (≈ 80 percent). identical D1-fragments emit similar continuum γ -ray spectra which rotational properties. As a consequence, both of the essentially because large amounts of angular momentum can be transferred into the intrinsic spin of these nuclei, which are known to have good reaction $^{18}\text{O} + ^{16}\text{O} \rightarrow ^{15}\text{O} + ^{16}\text{O}$. This system was chosen An interesting measurement has been carried out for the

4c) APPLICATION TO EXPERIMENTAL γ -RAY ANGULAR DISTRIBUTIONS

is the Dawson's integral. One can verify immediately that both expressions behave as expected in the limits of $\lambda = 0$ and $\lambda = \infty$. The anisotropy $W(\theta)/W(90^\circ)$ tends to 1 when λ tends to infinity both for E1 and E2 transitions, while it tends to 0 for E2 and to 2 for E1 when $\lambda = 0$.

$$F(x) = e^{-x^2} \int_0^x e^{t^2} dt$$

In these equations $\lambda = \sigma/I_2$ and $D(\lambda) = \sqrt{2} \lambda F(1/\sqrt{2} \lambda)$ where

$$W(\theta)_{E2} = \frac{4}{5} [1 - \cos^2 \theta - 2\lambda^2 \{3 \sin^2 \theta \cos^2 \theta - 2 \cos^4 \theta + \frac{4}{3} D(\lambda) (\sin^2 \theta - 4 \cos^2 \theta) \sin^2 \theta\} + 3\lambda^4 \{4 \cos^4 \theta + \frac{2}{3} \sin^4 \theta - 12 \sin^2 \theta \cos^2 \theta\} (1 - D(\lambda))] \quad (27)$$

For the E2 distribution one obtains:

$$W(\theta)_{E1} = \frac{4}{3} [1 + \cos^2 \theta + \lambda^2 (1 - D(\lambda)) (1 - 3 \cos^2 \theta)] \quad (26)$$

For the E1 distribution one obtains:

Fig. 11. Experimental and calculated (solid line) anisotropies vs Q-value. The dashed line shows the effect of E1 gamma rays alone and the dotted line shows the effect of neutron emission.

XBL814-2229

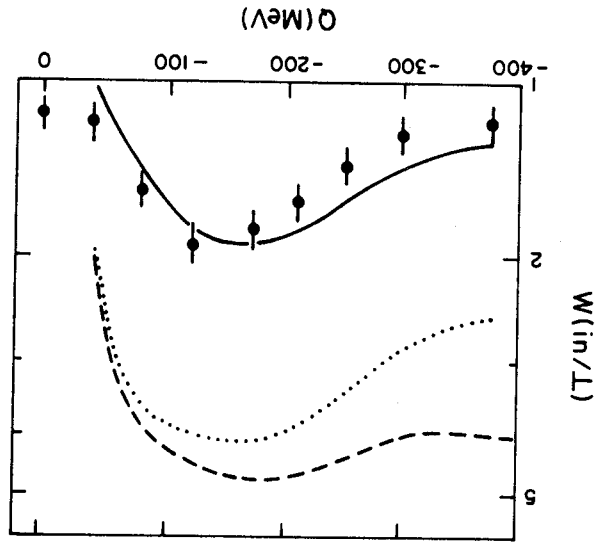
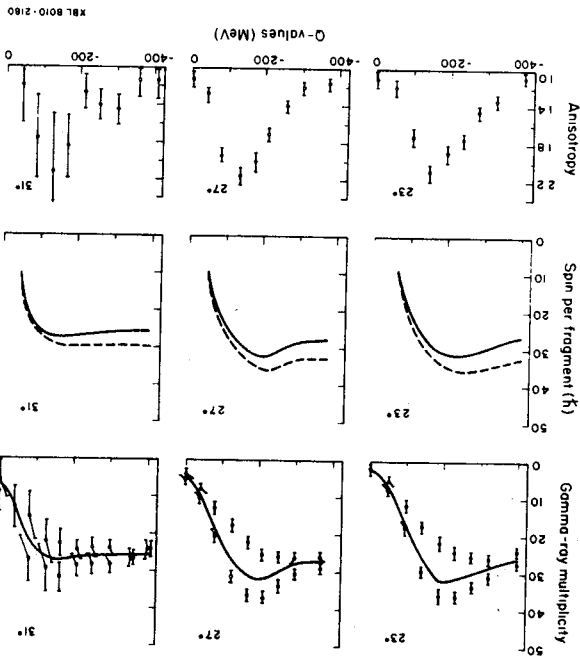


Fig. 10. Top: in-plane, out-of-plane (data points) and integrated γ -ray multiplicity as a function of Q-value for the reaction $\text{Ho} + \text{Ho}$ at 8.5 MeV/A. Middle: spin per fragment before (dashed curve) and after (solid curve) neutron emission as a function of Q-value. Bottom: gamma-ray anisotropy as a function of Q-value.



XBL 8010-2180

In most cases K_2^0 is fairly large, or at least comparable with

$$(30) \quad \frac{W(\phi = 90^\circ)}{W(\phi = 0^\circ)} = \left(\frac{K_2^0 + \sigma_z^2}{K_2^0 + \sigma_y^2} \right)^{1/2}$$

The quantity J_n is the moment of inertia of the nucleus after neutron emission, $J_{||}$ and J_{\perp} are the parallel and the perpendicular moments of inertia of the critical shape for the decay (e.g., saddle point), $J_{||}^0$ and J_{\perp}^0 is the temperature. The angular momentum dependence of the particle/neutron competition or fission/neutron competition is explicitly taken into account through β . It is worthwhile considering the in-plane anisotropy:

$$(29) \quad \beta = \frac{h^2}{2\pi} \left(\frac{J_{\perp}^0}{J_{||}^0} - \frac{J_{\perp}^1}{J_{||}^1} \right), \quad K_2^0 = \left(\frac{J_{||}^0}{J_{||}^1} - \frac{J_{\perp}^0}{J_{\perp}^1} \right)^{-1} \frac{h^2}{2\pi}$$

$$A_{mx} = I_2 \left[\frac{\cos^2 \theta}{2S^2} - \beta \right]; \quad A_{min} = I_2 \left[\frac{\cos^2 \theta}{2S^2} - \beta \right]$$

$$S^2(\theta, \phi) = K_2^0 + (\sigma_x^2 \cos^2 \phi + \sigma_z^2 \sin^2 \phi) \sin^2 \theta + \sigma_y^2 \cos^2 \theta$$

where

$$(28) \quad W(\phi, \theta) = \frac{1}{S} \left[\frac{I_2}{A_{min}} \exp(-A_{min}) - \frac{I_2}{A_{mx}} \exp(-A_{mx}) \right]$$

The magnitude of the transferred angular momentum and of its misalignment can be measured through the in- and out-of-plane angular distribution of sequentially emitted products. The angular distribution of fission fragments and of light particles emitted by a compound nucleus can be described in terms of a single theory.^{4,17} The product angular distribution in the two angles ϕ (in-plane) and θ (out-of-plane) is given by:

4d) ANGULAR DISTRIBUTIONS OF SEQUENTIAL FISSION AND OF SEQUENTIAL LIGHT PARTICLE EMISSION

The spin I was determined from the γ -ray calculation. The anisotropy was then calculated (solid line). This calculation reproduces both the shape and the magnitude of the data. To give a feeling for the importance of various contributions, the same calculation is shown including only E1 transitions (dashed curve) and including E1 transitions and neutron emission (dotted line). This comparison clearly shows that the most important effect is the thermally induced misalignment, indicating that the decrease of alignment as deduced from the anisotropy is inherent to the deep-inelastic process itself. A provisional conclusion is that the equilibrium statistical limit is very close to the regime controlling the spin misalignment in this reaction.

Fig. 12. The statistical widths for the normal modes of the dinuclear complex are shown as a function of mass asymmetry of the complex. The mass asymmetries associated with recent measurements of the angular distributions are also shown.

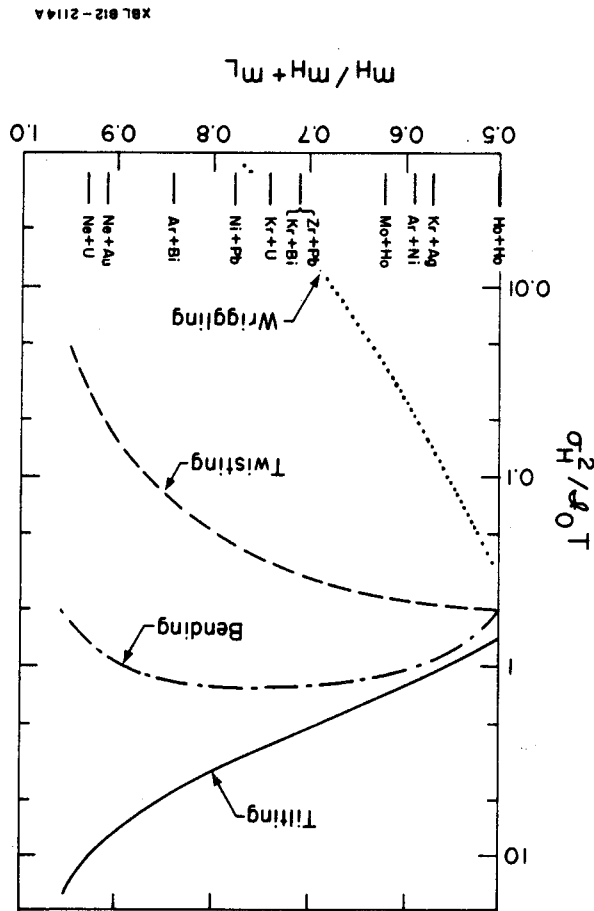
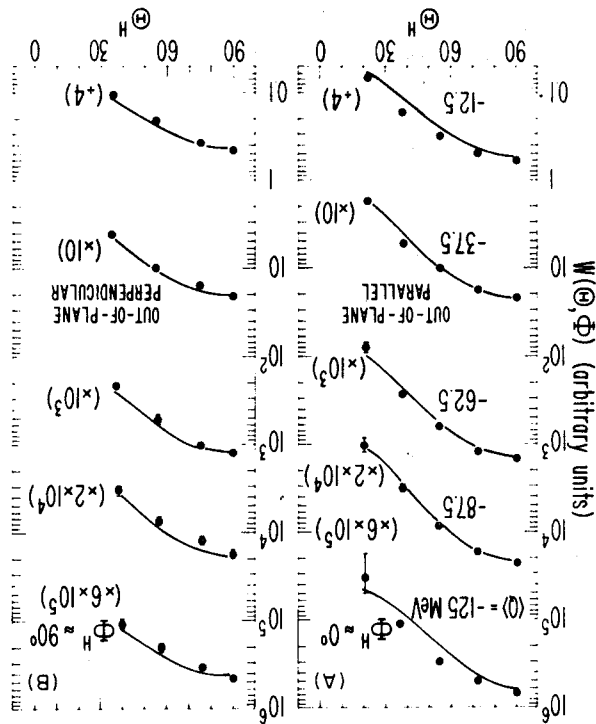


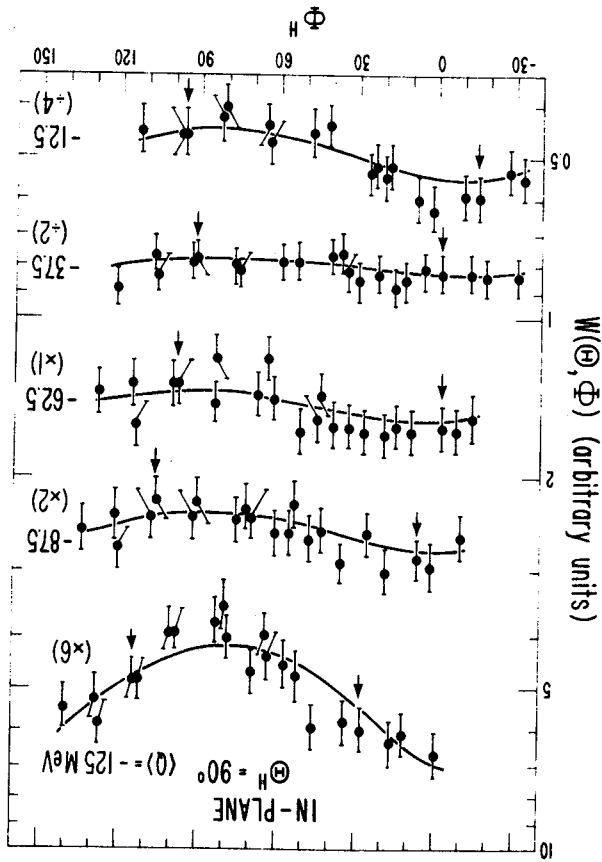
Fig. 13. The in-plane angular distributions of sequential fission fragments in the rest frame of the heavy fragment (H) are shown as a function of reaction Q-value for the $^{20}\text{Ne} + ^{238}\text{U}$ system. The arrows indicate the in-plane angles at which out-of-plane measurements were made. The solid curves are obtained by fitting the eq. 28 to the data in each Q-value bin.



The measured angular distributions are presented in figs. 13, 14 for the $^{20}\text{Ne} + ^{238}\text{U}$ system as a function of Q-value. The data have been integrated over the fission fragment energy and the atomic number of projectile residues ($6 \leq Z \leq 14$). The direction $\Phi_H = 0$ was arbitrarily chosen to coincide with the laboratory recoil angle as is traditional. The sequential fission events observed at small Q-values have a small in-plane anisotropy. The anisotropy disappears at intermediate Q-values; however, for the most inelastic collisions a strong minimum is seen approximately perpendicular to the lab recoil direction. Statistically significant angular distributions from reactions with ^{197}Au were obtained only at large Q-values. The position of the minimum and the anisotropies of these angular distributions are essentially the same as those shown for the most inelastic ^{238}U data.

In order to extract quantitative values for the spin polarization of the heavy fragment we have fit the angular distribution data with eq. (28). Finally, one must determine the direction of the line-of-centers of the intermediate complex at the time of separation with respect to the traditional reference direction, the laboratory recoil angle. In the limit of a nearly

Fig. 14. The out-of-plane angular distributions that correspond to the Φ -bins of fig. 13 are shown (solid points) along with the fitted functions (solid curves).
 elastic collision, without loss of orbital angular momentum, the two directions coincide. But whenever there is a decrease in orbital angular momentum between the entrance and exit channels, in the limit of zero orbital angular momentum corresponds to the laboratory system. In the limit of zero orbital angular momentum in the exit channel, the line-of-centers corresponds to the direction of the recoil in the center-of-mass system. The direction of the line-of-centers should vary for the data presented in figs. 13 and 14 from nearly equal to the lab recoil direction at $Q = -12.5$ MeV to approximately perpendicular to the lab direction at $Q = -150$ MeV! We have allowed for such a shift in the zero point of the angular distribution by another free parameter in the fitted function. This shift parameter, χ_{HF} , was only constrained to be near 0° for the nearly elastic bin and near 90° for the most inelastic bins. The results of chi-squared minimization fitting (K_0 values following ref. 21) are shown by the solid curves in figs. 13 and 14 and are contained in Table 1.



This work was supported by the Director, Office of Energy Research, Division of Nuclear Physics of the Office of High Energy and Nuclear Physics and by Nuclear Sciences of the Basic Energy Sciences Program of the U.S. Department of Energy under Contract W-7405-ENG-48.

In this brief review we have tried to show the relevance of statistical fluctuations to the understanding of a variety of aspects associated with deep inelastic processes. We have argued that, in several instances where there is evidence for extensive relaxation, one can use the equilibrium thermal widths as good estimates of the actual widths. Several tests are also suggested, and specific predictions based upon the equilibrium statistical limit are made. The present analysis suggests that the equilibrium statistical limits are extremely useful and should be employed to verify that the predictions of specific nonequilibrium models and their agreement with experiment are not solely associated with their correct long time limit. At present, it is possible to conclude tentatively that, while the whole of the deep inelastic process is clearly a nonequilibrium event, many of the involved degrees of freedom appear to have undergone a substantial relaxation compatible with a description in terms of statistical equilibrium.

5. Conclusion

The quantitative predictions of the statistical model are given in Table 1 for the most inelastic bin where we expect the model to be valid. In general, the agreement is quite good. Also the evolution of the anisotropy of the in-plane angular distributions with Q -value are in agreement with our expectations that the statistical model is valid in the long time limit.

Q Value (MeV)	K_0	I_z	0_x	0_y	0_z	Statistical model
-12.5	7.3	17.7(0.5)	3.0(0.6)	6.5(0.4)	2.8(0.4)	8.(7.)
-37.5	10.4	27.2(0.2)	7.7(0.2)	8.8(0.2)	1.9(0.5)	16.(9.)
-62.5	12.0	31.1(0.3)	9.5(0.5)	5.8(0.7)	3.1(0.7)	90.(9.)
-87.5	13.1	37.9(0.3)	13.0(0.7)	8.6(0.9)	5.3(0.5)	94.(9.)
-125.	16.3	42.4(0.6)	20.0(0.7)	0.7(4.)	9.2(1.1)	80.(3.)
-125.			24.1	8.7	8.7	80°

Table 1. Results of angular distribution fitting including the rotation angle χ_{HP} , errors are given in parenthesis.

- 1) R.A. Broglia, R.A. Civitarese, C.H. Dasso, and Aa. Winther, Phys. Lett. 73B (1978) 405
- 2) See for instance: L.G. Moretto, C.R. Albigston and G. Mantzouranis, Phys. Rev. Lett. 44 (1980) 924
- 3) L.G. Moretto and R.P. Schmitt, Phys. Rev. C21 (1980) 204
- 4) L.G. Moretto, Nucl. Phys. A247 (1975) 211
- 5) B. Cauvin, R. Jared, P. Russo, R.P. Schmitt, R. Babinet, and L.G. Moretto, Nucl. Phys. A301 (1977) 511
- 6) F. Piasil, R.L. Ferguson, H.C. Britt, R.H. Stokes, B.H. Erkkila, P.D. Goldstone, M. Blann and H.H. Gutbrod, Phys. Rev. Lett. 40 (1978) 1164
- 7) R.P. Schmitt, G. Bizard, G.J. Wozniak and L.G. Moretto, Phys. Rev. Lett. 41 (1978) 1152
- 8) B. Tamain, R. Chechik, H. Fuchs, F. Hanappe, M. Morjean, C. Ngô, J. Peter, M. Dakowski, B. Lucas, C. Mazur, M. Ribrag and C. Signarbieux, Nucl. Phys. A330 (1979) 253
- 9) Y. Eyal, A. Gavron, I. Tseruya, Z. Fraenkel, Y. Eisen, S. Wald, R. Bass, C.R. Gould, G. Kreyling, R. Renfordt, K. Stelzer, R. Zitzmann, A. Gobbi, U. Lynen, H. Stelzer, I. Rude and R. Bock, Phys. Rev. Lett. 41 (1978) 625
- 10) D. Hilscher, J.R. Birkelund, A.D. Hoover, W.U. Schröder, W.W. Wilcke, J.R. Huizenga, A. Mignerey, K.L. Wolf, H.F. Breuer, and V.E. Viola, Jr., Phys. Rev. C20 (1979) 576
- 11) L.G. Moretto, Proc. Varenna Conf., Varenna, Italy, July 9-25, 1979, in press.
- 12) R.P. Schmitt, G.J. Wozniak, G.V. Rattazzi, G.J. Mathews, R. Regimbat and L.G. Moretto, Phys. Rev. Lett. 46 (1981) 522
- 13) M. Berlangier, A. Gobbi, F. Hanappe, U. Lynen, C. Ngô, A. Olmi, H. Sann, H. Stelzer, H. Richel and M.F. Rivet, Z. Phys. A291 (1979) 133
- 14) J. Poltou, R. Lucas, J.V. Kratz, W. Bruchle, H. Gaggeler, M. Schadel, and G. Wirth, Phys. Lett. 88B (1979) 69
- 15) A.C. Mignerey, V.E. Viola, H. Breuer, K.L. Wolf, B.G. Glagola, J.R. Birkelund, D. Hilscher, J.R. Huizenga, W.U. Schröder and W.W. Wilcke, Phys. Rev. Lett. 45 (1980) 509
- 16) D.J. Morrissey and L.G. Moretto, Phys. Rev. C23 (1981) 1835
- 17) L.G. Moretto, S. Blau and A. Pacheco, Nucl. Phys. A364 (1981) 125

References

- 18) G.J. Wozniak, R.J. McDonald, A. Pacheco, C.C. Hsu, D.J. Morrissey, L.G. Sobotka, L.G. Moretto, S. Shin, C. Schuck, R.M. Diamond, H. Kluge, and F.S. Stephens, Phys. Rev. Lett. 45 (1980) 1081
- 19) D.J. Morrissey, G.J. Wozniak, L.G. Sobotka, A.J. Pacheco, C.C. Hsu, R.J. McDonald and L.G. Moretto, LBL-12181 (March 1981)
- 20) L.G. Sobotka et al., Phys. Rev. Lett. in press (1981)
- 21) P. Dyer et al., *ibid* 39 (1977) 392 and Nucl. Phys. A322 (1979) 205
- 22) R.J. Puigh et al., Phys. Lett. 86B (1979) 24
- 23) D. v. Harrach et al., Phys. Rev. Lett. 42 (1979) 1728
- 24) C. Lebrun et al., 6th Session d'Etudes Biennale de Physique Nucleaire, Aussis, France, 2-6 February 1981

1
2
3
4
5
6
7

1
2
3